Multi-objective shape optimization of submarine hull using genetic algorithm integrated with computational fluid dynamics

Article *in* Proceedings of the Institution of Mechanical Engineers Part M Journal of Engineering for the Maritime Environment · June 2017

DOI: 10.1177/1475090217714649

CITATIONS
0

READS
297

3 authors:

Kondeti Lakshmi Vasudev
Hindustan University
16 PUBLICATIONS **38** CITATIONS
SEE PROFILE

R. Sharma
Indian Institute of Technology Madras
52 PUBLICATIONS **122** CITATIONS
SEE PROFILE

Subrata Bhattacharya
Indian Institute of Technology Madras
97 PUBLICATIONS **451** CITATIONS
SEE PROFILE

Original Article

Institution of MECHANICAL ENGINEERS

Journal of ENGINEERING FOR THE MARITIME ENVIRONMENT

Proc IMechE Part M:
J Engineering for the Maritime Environment
1–12

DOI: 10.1177/1475090217714649
journals.sagepub.com/home/pim
SAGE

Multi-objective shape optimization of submarine hull using genetic algorithm integrated with computational fluid dynamics

K. L. Vasudev, R. Sharma and S. K. Bhattacharyya

Abstract

A multi-objective optimization framework is developed for design of submarine hull shape. Internal volume of the vehicle and its hydrodynamic drag are optimized by seamlessly integrating non-dominated sorting genetic algorithm and Reynolds averaged Navier–Stokes solver in a single code. The methodology seeks a geometric shape with minimum drag and maximum volume satisfying the constraints on the geometric design parameters given by a 5-parameter formula that describes the submarine hull. The shape of the sail is not a part of the optimization process, and only its longitudinal location over the submarine hull is optimized. Two design optimization approaches are proposed, solved and compared. In the first approach, the combined hull–sail location is optimized, and in the second, the hull shape without sail is optimized first, and for this optimized hull shape, the sail location is optimized next. Our reported results show that the former approach yields significantly lower drag.

Keywords

Computational fluid dynamics, drag, genetic algorithm, submarine

Date received: 8 July 2016; accepted: 5 May 2017

Introduction

The minimization of power requirements of underwater vehicles is a central objective in their design, and it is an important problem in the area of marine hydrodynamics. The power reduction is accomplished, in general, by some combination of shaping the hull, controlling the boundary layer by polymer injection, slot suction and so on, adopting energy-saving propulsion system such as a wake adopted propeller or a suction slot with a stern jet, and using efficient maneuvering system consistent with hydrodynamic stability. The first two of this list attempt to reduce skin friction and pressure drag while the third attempts to reduce the energy that is lost to the fluid. A complete systems design simultaneously takes into account all these aspects although the complex nature of the complete problem does not permit analytical systems design approach.[1]

In this article, an approach to the automatic synthesis of minimum drag hull shapes for axisymmetric underwater vehicles at specified forward speed and enclosed volume is presented. The multi-objective optimization procedure developed in this work makes use of genetic algorithms (GAs) for optimization and computational fluid dynamics (CFD) for the evaluation of the objective function which is of hydrodynamic origin (i.e. drag) in order to arrive at a desired hull shape of a vehicle. The approach is demonstrated with the example of an axisymmetric submarine hull with its sail structure. The specification of the problem is such that it aims to achieve minimum hydrodynamic drag at the desired forward speed with constraints on shape parameters considering the longitudinal position of the sail as an optimization variable. With rapid development of computational tools in the recent years, CFD and advanced optimization techniques have started to play an important role in the computer-aided geometric design (CAGD) of underwater vehicles.

Department of Ocean Engineering, Indian Institute of Technology Madras, Chennai, India

Corresponding author:
K. L. Vasudev, Department of Mechanical Engineering, Hindustan University, Chennai 603103, Tamilnadu, India.
Email: lakshmivasudev.k@gmail.com

A multi-criteria optimization model using simulated annealing technique to optimize the ship design process was used by Ray et al.[2] to automate the design process of marine vehicles where the decision system was based on an analytic hierarchy process. Warren[3] studied submarine hull designs described by parametric formulae for nose, middle body and stern regions using Reynolds averaged Navier–Stokes (RANS) equations with a vortex lattice propeller design code to obtain preliminary hull forms. Percival et al.[4] implemented a downhill simplex method on classical Wigley hull for a range of velocities with constraints on the displacement and transverse moment of area of waterplane to minimize drag. The hull surface was defined by nonuniform rational B-splines and the drag evaluations were carried out using the ITTC formula for frictional resistance and zeroth-order slender ship approximation for wave resistance. Campana et al.[5] developed two approaches of optimization, namely, "narrow band derivative-free" approach and "variable fidelity" approach. CFD was used to evaluate the total drag of the ship (objective function), and the results were validated by conducting model tests. Similar work was done by Peri and Campana[6] and Tahara et al.[7]

Demko[8] studied the practical and quantitative methods of multi-objective and multi-disciplinary optimization to estimate their effectiveness in naval ship design. A method was presented that uses the analytic hierarchy process combined with multi-attribute value theory to build an overall measure of effectiveness and an overall measure of risk function in order to rank and approximately measure the relative mission effectiveness and risk of design alternatives, taking the aid of trained expert opinion to replace complex analysis tools. Hart and Vlahopoulos[9] developed a multi-disciplinary design optimization approach for the design of submarine considering four objectives, namely, deck area, resistance, structural design and maneuvering. Length of the parallel middle body, maximum diameter, tail shape parameter and nose shape parameter were used as design variables. However, a single objective was treated at a time for optimization using particle swarm optimization (PSO) technique. Therefore, it is essentially a single objective optimization problem. All objective function evaluations were done by semi-empirical formulae. Shahid and Huang[10] implemented GA-based optimization in the design of bulbous bow of series 60 hull using a potential flow solver to evaluate the total resistance of the ship.

Paz and Tascon[11] implemented multi-objective optimization based on GA for submarine, where the main objectives were to minimize the nondimensional steady turning diameter and the resistance at maximum speed. They used empirical relations[12,13] to evaluate the total resistance and used semi-empirical relations to compute hydrodynamic derivatives of the bare hull, sail and control surfaces as given by Mackay.[14] The design variables were hull length, hull diameter, nose and tail shape coefficients, longitudinal location of the sail, rudder area and rudder aspect ratio.

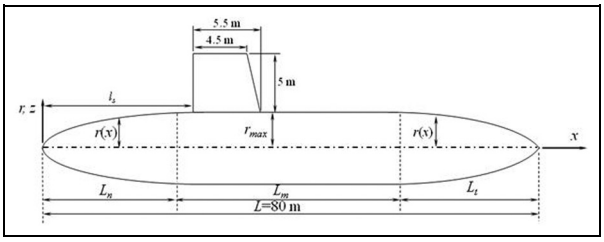

Figure 1. Parameterization of the hull geometry.

Vasudev et al.[15] developed a non-dominated sorting genetic algorithm (NSGA-II)-based multi-objective optimization framework using RANS solver to obtain an optimum hull form of an autonomous underwater vehicle (AUV). The objectives were to minimize the drag and maximize the wake fraction and volume.

The main objective of this work is to develop a multi-objective optimization framework that can be useful in the conceptual design phase of the development of hydrodynamically efficient shapes of submarines with sail structure. The optimization problem involves minimization of hydrodynamic drag and maximization of volume subject to the constraint that the overall length must be constant. The submarine shape is assumed to be axisymmetric and is described by a 5-parameter formula.[16] The multi-objective optimization technique NSGA-II[17,18] has been adopted in this work. The main focus of this work is to seamlessly integrate the implementation of NSGA-II developed in MATLAB with a commercially available steady-state RANS solver Shipflow.[19] In other words, the GA code, mesh generator and steady-state RANS solver are integrated so as to eliminate user intervention during the optimization process.

Geometry definition

The geometry of the submarine is axisymmetric and is shown in Figure 1. The parameterized shape is given by[16]

$$r(x) = \begin{cases} r_{max}\left(1 - \left(\frac{L_n - x}{L_n}\right)^{n_n}\right)^{1/n_n} & \text{for } 0 \leqslant x \leqslant L_n \\ r_{max} & \text{for } L_n \leqslant x \leqslant L_n + L_m \\ r_{max}\left(1 - \left(\frac{x - L_n - L_m}{L_t}\right)^{n_t}\right) & \text{for } L_n + L_m \leqslant x \leqslant L \end{cases}$$
$$L_n + L_m + L_t = L \tag{1}$$

where r_{max} is the maximum radius of the body so that the maximum diameter is d_{max} ($= 2r_{max}$) and a middle body length L_m has this radius; $r(x)$ is the variation of radius over the total length L; L_n and L_t are the lengths of the nose and the tail, respectively; and the exponents n_n and n_t are associated with the nose and tail shapes respectively.

The shape given by equation (1) leads to a conical nose shape (i.e. linear $r(x)$) for $n_n = 1$ and a conical tail shape for $n_t = 1$. For large values of n_n, the nose shape profile approaches a rectangle (i.e. $r(x)$ approaches r_{max}) and similarly, for large values of n_t, the tail shape profile also approaches a rectangle. For $n_n < 1$ and $n_t < 1$, the nose and tail shapes reverse the sign of their curvatures.

In numerical examples, the length (L) of the submarine is always kept constant at 80 m. The sail size and shape also is constant and consists of tapered NACA0012 profile with a root chord length of 5 m, tip chord length of 4 m and a span of 4.5 m. The longitudinal location of the sail (l_s, see Figure 1) is one of the design variables in the optimization problem. The volume (∇), a design variable, is

$$\nabla = \pi \int_0^L r^2(x)dx \tag{2}$$

Drag model

The hydrodynamic drag (D) is computed by steady-state RANS approach and can be expressed as

$$\mathrm{D} = \frac{1}{2}\rho C_{DV} U^2 \nabla^{2/3} = D_f + D_{pv} = \frac{1}{2}\rho C_{FV} U^2 \nabla^{2/3} + \frac{1}{2}\rho C_{PV} U^2 \nabla^{2/3} \quad (C_{DV} = C_{FV} + C_{PV}) \tag{3}$$

where ρ is the density of the water, C_{DV} is the volumetric drag coefficient, ∇ is the volume of the hull (without sail), C_{FV} is the volumetric frictional drag coefficient and C_{PV} is the volumetric viscous pressure drag coefficient. Steady-state RANS solver evaluates both the frictional drag D_f and the total drag (D) so that the viscous pressure drag D_{pv} is also known for a particular velocity (U).

The computational domain is shown in Figure 2 where S_B is the body boundary, S_1 is the surface enclosing the submarine hull without the sail which is close to S_B and S_2 is the surface of enclosing the sail which is close to S_B. The surface S encloses the full computational domain spanning $-L_1 \leqslant x \leqslant L + L_2$, $-L_3 \leqslant y \leqslant L_3$ and $-L_3 \leqslant z \leqslant L_3$ so that the enclosed domain is a cuboid of length $L_1 + L + L_2$, breadth $2L_3$ and height $2L_3$. The values $L_1 = 0.7L$, $L_2 = 4.5L$ and $L_3 = 0.6L$ ($L = 80$ m) were adopted in all calculations, since from convergence study, these choices have been found more than sufficient to capture the entire viscous–inviscid interaction and the wake development. It should be noted that the domain within S, domain between S_B and S_1 and domain between S_B and S_2 are meshed independently. The steady-state RANS solver automatically generates interface information between the meshes of these three domains and uses it in the solver. This capability is critical in meshing non-axisymmetric and complex body geometries.

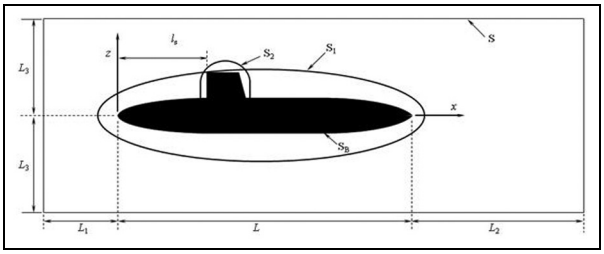

Figure 2. Computational domain and its boundaries.

The domain between S_B and S_1 has a graded mesh with growth ratio ($= g$) starting with the grid point nearest to S_B (wall adjacent cell size) located at a (perpendicular) distance of l_1 from S_B ensuring

$$l = \sum_{i=1}^{N_r} l_1 g^{i-1} \tag{4}$$

where N_r is the number of cells between S_B and S_1 in the direction normal to S_B spanning a length l. This ensures that the mesh generated is an H-type structured mesh. The growth ratio (g) should be so chosen that it prevents the cells adjacent to the wall from being placed in the buffer layer of $y^+ = 1$. The acceptable distance between the cell centroid and the cells adjacent to the wall is usually measured in the wall unit $y^+ = yu_\tau/U$, where $u_\tau = \sqrt{\tau_w/\rho}$ is the friction velocity and τ_w is the wall shear stress. However, it requires some trial and error to determine a suitable value of l_1.

The surface S_1 has N_x cells along its length direction (i.e. x direction) and N_θ cells in the circumferential direction which are at equal angles apart. Thus, there are $N_x \times N_r \times N_\theta$ cells in the domain between S_B and S_1 such that the distance between S_B and S_1 is constant ($= l$) everywhere. The mesh between S_B and S_1 is, therefore, completely defined once l_1, g, N_x, N_r and N_θ are specified.

The domain between S_B and S_2 has a similar H-type structured mesh but defined by another set of values of l_1 and g in the direction along the ray of length l normal to the surface of the sail yielding N_r cells, in the circumferential direction of the sail yielding N_θ cells and in the longitudinal direction along the span of the sail yielding N_x cells. The mesh in the rectangular box with surface S consists of uniform mesh ($g = 1$) in all three directions with N_x, N_y and N_z cells in x, y and z directions, respectively.

The mesh sensitivity study was conducted considering various values of N_x, N_r, N_θ, l, and g in the domain between S_B and S_1, and various values of N_x, N_y and N_z in the domain S. In all cases, the mesh parameters between S_B and S_2 were kept same, namely, $l_1 = 1$ mm, $g = 1.2$ and $N_x \times N_r \times N_\theta = 63 \times 30 \times 30$. For these chosen mesh parameters, corresponding y^+ and C_{DV} values are recorded in Table 1. It is evident from Table 1 that there is no significant difference in C_{DV} between the mesh with 1.8 million cells and one with 2.7 million

Table 1. Grid sensitivity study.

Total no. of cells (million)	g	l (m)	$N_r \times N_\theta \times N_x$ (between S_B and S_1)	$N_x \times N_y \times N_z$ (in S)	y^+	C_{DV}	% change in C_{DV} with respect To previous grid
H1-S1							
1.2	1.12	3.81	$90 \times 115 \times 51$	$170 \times 61 \times 61$	0.7	0.020967	
1.8	1.1	6.24	$90 \times 140 \times 51$	$200 \times 71 \times 71$	0.2	0.018397	13.9
2.7	1.09	10.81	$90 \times 160 \times 51$	$250 \times 77 \times 77$	0.179	0.018621	1.2
3.5	1.08	19.07	$90 \times 185 \times 51$	$300 \times 85 \times 85$	0.177	0.018479	−0.7
6.1	1.06	8.235	$90 \times 225 \times 51$	$500 \times 97 \times 97$	0.172	0.018447	−0.18
H2-S2							
1.8	1.1	6.24	$90 \times 140 \times 51$	$200 \times 71 \times 71$	0.2	0.02212	
2.7	1.09	10.81	$90 \times 160 \times 51$	$250 \times 77 \times 77$	0.107	0.01952	11.75
3.5	1.08	19.07	$90 \times 185 \times 51$	$300 \times 85 \times 85$	0.096	0.01945	0.35

cells. Therefore, the mesh with 1.8 million cells has been used in all calculations. However, the drag of the final optimized configuration is obtained from the mesh with 3.5 million cells to achieve high accuracy. A typical mesh is shown in Figure 3.

The shear stress transport or SST k–ω turbulence model, where k is the turbulent kinetic energy and ω is the specific dissipation rate, was adopted for the closure of RANS equations. On the boundary S_B, the no-slip boundary condition, on the boundary at x $(= -L_1)$, the velocity inlet condition, where the velocity U is prescribed in the x direction, on the boundary at $x = L + L_2$, the pressure outlet condition, in other words, the pressure (p) is set to gauge pressure (i.e. $p = 0$) and the gradients of k and ω are set to zero and on the remaining boundaries at $y = \pm L_3$ and $z = \pm L_3$ of the domain inside S, zero shear stress condition has been imposed.

Optimization problems

The objective functions of the design optimization problems treated in this article are drag and volume of the submarine and the variables are the five shape parameters of the body (L_n, L_t, n_n, n_t and r_{max}, see equation (1)) and the longitudinal location of the sail (l_s, see Figure 1). The sail geometry is fixed and only its location is treated in the optimization process. We define

$$\begin{aligned} &F_1 = D(\text{drag, see equation(3)}),\\ &F_2 = \nabla(\text{volume, see equation(2)})\\ &x_1 = L_n,\ x_2 = L_t,\ x_3 = n_n,\ \ x_4 = n_t,\\ &x_5 = r_{max},\ x_6 = l_s \end{aligned} \tag{5a}$$

where F_1 and F_2 are the objective functions and x_i (i = 1–6) are the design variables. The lower and upper bounds of the design variables are denoted as x_{Li} and x_{Ui}, respectively. In other words

$$x_{Li} \leqslant x_i \leqslant x_{Ui} \quad (i = 1, 2, \ldots, 6) \tag{5b}$$

The values chosen for these bounds are

$$\begin{aligned} &x_{L1} = x_{L2} = 5\text{ m},\ x_{L3} = x_{L4} = 1,\ x_{L5} = 3\text{m},\ x_{L6} = 15\text{m}\\ &x_{U1} = x_{U2} = 40\text{m},\ x_{U3} = x_{U4} = 5, x_{U5} = 4\text{m},\ x_{U6} = 60\text{m} \end{aligned} \tag{5c}$$

The total length of the submarine (L) is constant at 80 m. This is an equality constraint in the optimization problem given by (see Figure 1)

$$L_m + x_1 + x_2 = L \tag{5d}$$

The three optimization problems, all subject to the variable bounds given by equation (5b) with their values given in equation (5c) and the equality constraint equation (5d), have been treated in this article. These are as follows:

1. *Problem P1*. Minimize $F_1(x_1, \ldots, x_6)$ and maximize $F_2(x_1, \ldots, x_6)$. This problem, involving six design variables, five for the submarine hull shape and one for the sail location, aims to find the optimum shape of the submarine and the optimum longitudinal location of the sail.
2. *Problem P2*. Minimize $F_1(x_1, \ldots, x_5)$ and maximize $F_2(x_1, \ldots, x_5)$. This problem, involving five design variables for the submarine hull shape, aims to find the optimum shape of the submarine without the presence of the sail.
3. *Problem P3*. Minimize $F_1(x_6)$. This problem with one objective function involves one design variable, which is the sail location, and it aims to find the optimum longitudinal location of the sail when the submarine hull shape parameters x_1 to x_5 are prescribed.

At this stage, it should be noted that the problem "Minimize $F_1(x_1, \ldots, x_5)$ and maximize $F_2(x_1, \ldots, x_5)$" is equivalent to "Minimize $F_1(x_1, \ldots, x_5)$ and minimize $c - F_2(x_1, \ldots, x_5)$" where c is a constant. In all numerical work, $c = \pi x_{U5}^2 L$ $(= 4021\,\text{m}^3)$ is assumed which is the volume of the cylinder of length L (i.e. length of the submarine) and radius x_{U5} (i.e. maximum permissible radius given by the upper bound of r_{max}) so that the function $c - F_2(x_1, \ldots, x_5)$ is always positive.

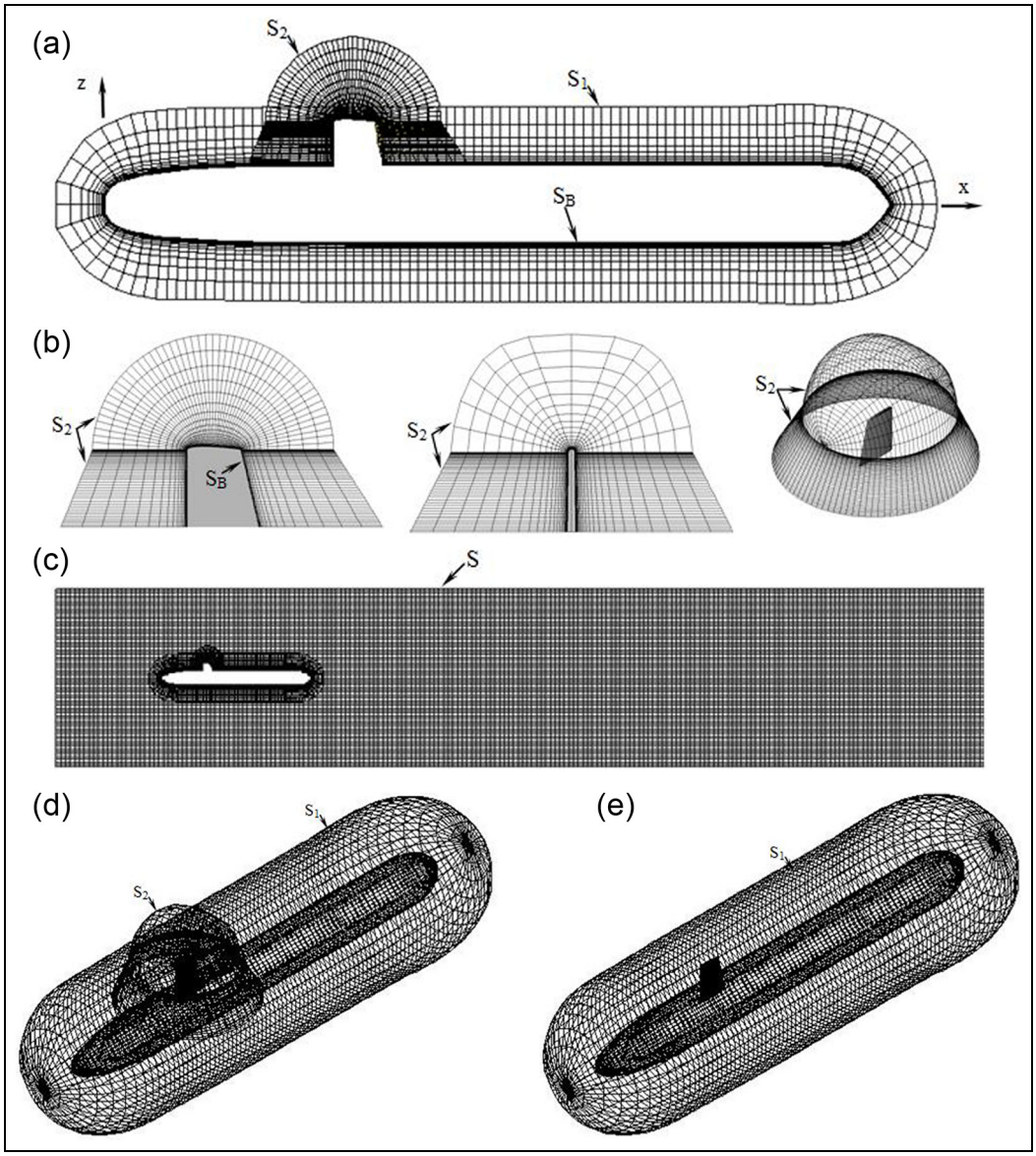

Figure 3. Mesh in the computational domain: (a) side view of mesh close to S_B showing S_1 and S_2 boundaries, (b) mesh between S_B and S_2, (c) mesh in the domain S, (d) mesh between S_B, S_1 and S_2 and (e) mesh between S_B and S_1.

Solution by GA

The method used to solve the linear equality constraint of equation 5(a) is the genetic algorithm for numerical optimization for constrained problems (GENOCOP) discussed in Michalewicz and Attia[20] and Miettinen et al.[21] The flowchart in Figure 4 provides an overview of GA-based optimization. The method, specialized to the problem given by equation (5), is discussed below.

Step 1: generate initial configurations

A vehicle configuration is given by the parameter set $x_i^{(j)}(i = 1, 2, \ldots, 6)$. We generate p vehicle configurations, with p even, denoted by $C^{(j)}$, where $j = 1$ to p, using

$$x_i^{(j)} = x_{Li} + \alpha(x_{Ui} - x_{Li}) \tag{6}$$

where α is a random number between 0 and 1 and is generated every time equation (6) is used. In other words, application of this equation requires generation of $6p$ random numbers.

We now have p vehicle configurations $C^{(j)}$ and in GA parlance, these configurations constitute the "initial population" and the parameter sets $x_i^{(j)}$ constitute p "chromosomes."

Step 2: sort initial configurations

We compute the drag forces ${F_1}^{(j)} = f^j$ by steady-state RANS solver and volume functions $c - {F_2}^{(j)} = g^j$ using equation (2) for each of these p configurations $C^{(j)}$. We rearrange these configurations using "non-dominated sorting (NS)" technique.[18] At the end of Step 2, we have p vehicle configurations $C_1^{(j)}$ which are sorted by NS

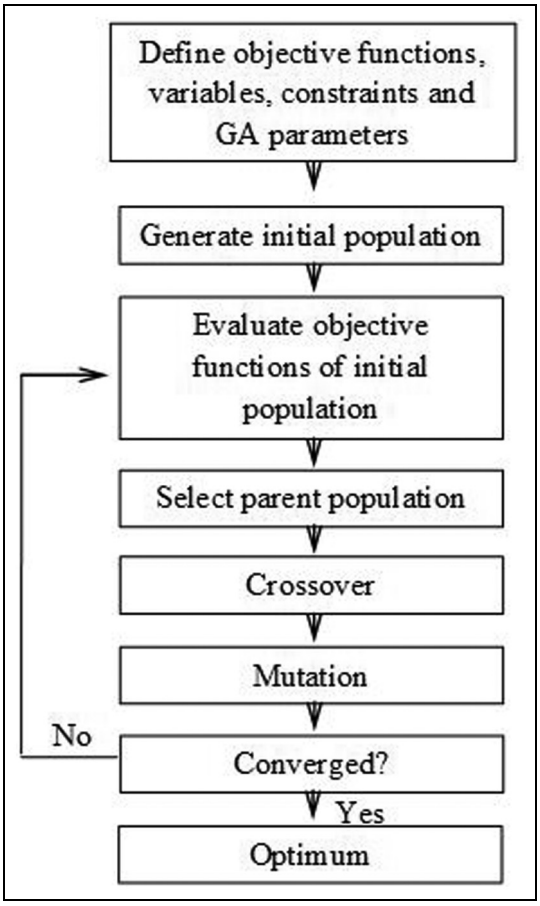

Figure 4. Flow chart of the optimization process using GA.

algorithm. This set of configurations, in GA parlance, is the parent population.

Step 3: generate configurations by crossover and mutation

Generate a random number α between 0 and 1. Set $l = 0$. Then, generate four random numbers $\beta_k (k = 1, \ldots, 4)$ between 0 and 1 and calculate

$$q_k = \text{nint}\left\{1 + \frac{(p-2)\beta_k}{2}\right\} \tag{7}$$

Arrange q_k in increasing order and relate them to β_k as follows

$$(q_k, \beta_k) \Rightarrow (\bar{q}_k, \bar{\beta}_k) \text{ such that } \bar{q}_1 \leqslant \bar{q}_2 \leqslant \bar{q}_3 \leqslant \bar{q}_4 \tag{8}$$

1. If $\alpha \leqslant \bar{\alpha}$, then generate two new configurations using

$$\begin{aligned} &l = l + 1;\ \bar{C}^{(l)} : x_i^{(l)} = \frac{1}{2}\left\{(1-\gamma_i)x_i^{(\bar{q}_1)} + (1+\gamma_i)x_i^{(\bar{q}_2)}\right\}; \\ &\text{exit Step 3 if } l = p \\ &l = l + 1;\ \bar{C}^{(l)} : x_i^{(l)} = \frac{1}{2}\left\{(1+\gamma_i)x_i^{(\bar{q}_1)} + (1-\gamma_i)x_i^{(\bar{q}_2)}\right\}; \\ &\text{exit Step 3 if } l = p \end{aligned} \tag{9}$$

where γ_i are random numbers between 0 and 1, generated each time the above two equations are used. Clearly, since there are six design variables, that is, $i = 1$–6, one would need 12 values of γ_i for these two configurations.

2. If $\alpha > \bar{\alpha}$, then generate one new configuration using

$$\begin{aligned} &l = l + 1;\ \bar{C}^{(l)} : x_i^{(l)} = x_i^{(\bar{q}_1)} + \delta(x_{Ui} - x_{Li}); \\ &\text{exit Step 3 if } l = p \end{aligned} \tag{10}$$

where

$$\begin{aligned} &\delta = (2\bar{\beta}_1)^{\frac{1}{\eta+1}} + 1 \text{ (if } \bar{\beta}_1 < 0.5); \\ &\delta = 1 - [2(1-\bar{\beta}_1)]^{\frac{1}{\eta+1}} \text{ (if } \bar{\beta}_1 \geqslant 0.5) \end{aligned} \tag{11}$$

In the above steps, we have used $p = 10$, $\bar{\alpha} = 0.8$ and $\eta = 20$.

At the end of Step 3, we have p vehicle configurations $\bar{C}^{(j)}$.

Step 4

We construct a set of $2p$ configurations by appending the set $\bar{C}^{(j)}$ to the set $C_1^{(j)}$ and denoting it as $\hat{C}^{(j)}$ where now, $j = 1$ to $2p$. In other words

$$< \hat{C} > = < C_1^{(1)}, C_1^{(2)}, \ldots, C_1^{(p)}, \bar{C}^{(1)}, \bar{C}^{(2)}, \ldots, \bar{C}^{(p)} >$$

We compute the drag forces F_1 by steady-state RANS solver and volumes F_2 using equation (2) for each of these p configurations $\bar{C}^{(j)}$. The values of F_1 and F_2 for configurations $C_1^{(j)}$ are already computed earlier in Step 2. Now, rearrange the configuration set $\hat{C}^{(j)}$ again using "non-dominated sorting (NS)" technique and retain the top p configurations as set $C_2^{(j)}$ with $j = 1$ to p.

Step 5

Rename $C_2^{(j)}$ as $C_1^{(j)}$ and go to Step 2 and continue till the end of Step 4. All configurations now lie on a converged (or optimal) Pareto front.

Numerical implementation

The focus of this work is on the coupling of GA implementation with a preprocessor and RANS solver. In other words, embedding the mesh generation and RANS solution in the computer implementation of the GA will lead the entire exercise to be carried out without any manual intervention during the entire optimization process.

In steady-state RANS solver calculations, the convergence of the total drag force (D) of the submarine with iterations is shown in Figure 5 for $U = 10$ m/s for a typical configuration. It can be seen that approximately 1500 iterations or more are required for

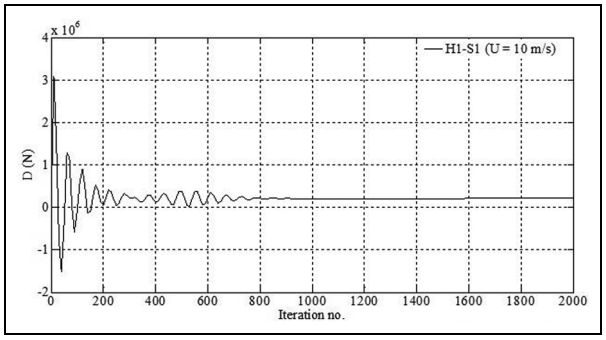

Figure 5. Steady-state RANS solver convergence of the total drag (D) for H1-S1 at $U = 10$ m/s.

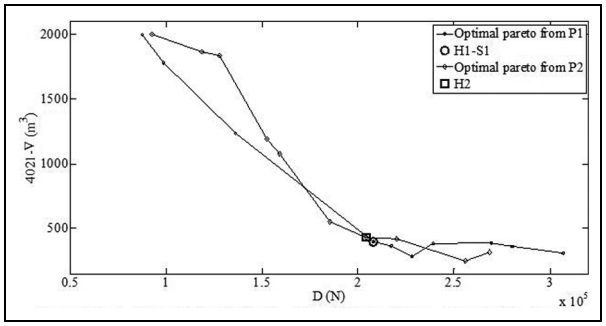

Figure 6. Pareto fronts obtained in Problem P1 and P2 after 16 generations for $U = 10$ m/s.

Table 2. The hull parameters of H1-S1 and H2-S2 ($U = 10$ m/s).

Parameters	H1-S1	H2-S2
L_n (m)	18.548	28.959
L_m (m)	48.772	42.093
L_t (m)	12.68	8.948
L (m)	80	80
r_{max} (m)	3.994	3.957
n_n	4.81	3.47
n_t	2.53	4.40
l_s (m)	50	22.92
S (m^2)	1962.19	1948.11
∇ (m^3)	3625	3592
L/D_{max}	10.01	10.11
$\nabla^{2/3}/S$	0.12	0.12
Re_L	7.97×10^8	7.97×10^8
C_{FV}	0.010467	0.01358
C_{PV}	0.007928	0.00854
C_{DV}	0.018396	0.02212
D (N)	215,965 (204,280[a])	260,949 (202,054[a])

[a]Drag of the hull (H1 or H2) without sail.

convergence. Therefore, in comparing the drag forces of many configurations as dictated by the GA scheme, the number of iterations was fixed at 2000, and the drag force has been obtained by its average over one cycle (between a peak and a trough) preceding the last iteration number. The drag of the final optimized configuration, however, is obtained from approximately 4000 to 6000 iterations to achieve high accuracy.

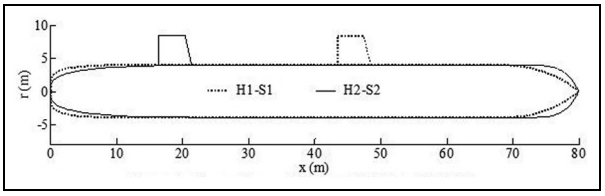

Figure 7. Comparison of shapes of H1-S1 and H2-S2.

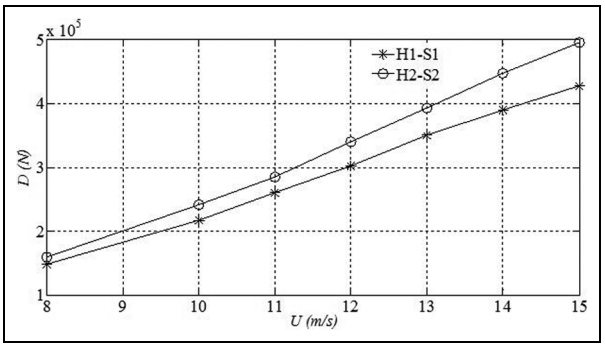

Figure 8. Drag curve of designs H1-S1 and H2-S2.

Results and discussion

Optimization problems P1, P2 and P3

The problem P1 (see section "Optimization problems") yields a design where the hull shape and the longitudinal location of the sail are optimized in a combined manner for $U = 10$ m/s. This optimized design is denoted H1-S1 indicating that its hull configuration is H1 and sail location is S1. The problem P2 yields a design where the hull shape is optimized for the same speed (i.e. $U = 10$ m/s) without considering the presence of the sail. This optimized design of the hull alone is denoted as H2. The optimal Pareto front for P1 and P2, a plot of total drag (D) and $c - \nabla (= \pi x_{U5}^2 L - \nabla = 4021 - \nabla)$, is presented in Figure 6. The problem P3 yields a design where the hull shape is H2 and the location of the sail alone is optimized at the same forward speed (i.e. $U = 10$ m/s). This optimized design is denoted H2-S2 where S2 indicates the sail location. The parameters of the two hulls H1 and H2 are presented in Table 2 and their shapes compared in Figure 7. The two hull shapes are picked from the optimal Pareto front such that the volumes of both the hulls are almost same (less than 1% of each other) as seen from Table 2.

The combined hull-sail optimized configuration H1-S1 has significantly lower drag (15% at $U = 10$ m/s) than the two-step hull-sail optimized configuration H2-S2. This underscores the importance of carrying out the optimization in a combined manner. The drag curves (D vs U) of the design H1-S1 and H2-S2 are shown in Figure 8. It shows that the drag of H2-S2 is higher than H1-S1 by 16.98% for $U = 8$ m/s and 45.6% for $U = 15$ m/s. In Table 2, drag of the

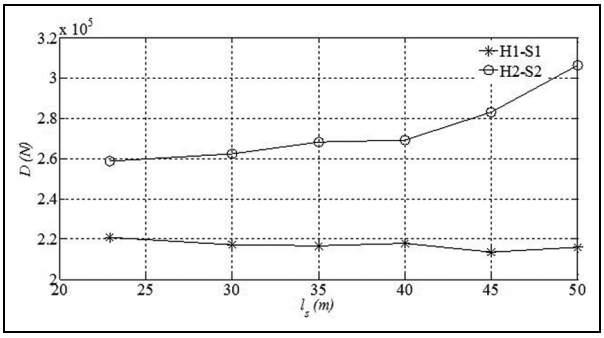

Figure 9. Drag of H1 and H2 for various locations of sail ($U = 10$ m/s).

submarine without sail is also given for both designs. It may be seen that whereas sail contributes 5.4% drag to the design H1-S1, it contributes 22.57% drag to the design H2-S2.

At $U = 10$ m/s, the drag values of H1-S1, H2-S2, H1-S2 and H2-S1 are 215,965, 260,949, 217,214 and 304,392 N, respectively. Since the drag values of H1-S1 (sail at $l_s = 50$ m) and H1-S2 (sail at $l_s = 22.92$ m) are very close (about 0.57% difference), despite the large difference in sail location, it suggests that location of sail does not have much influence on drag for the hull H1. On the other hand, the drag values of H2-S2 (sail at $l_s = 22.92$ m) and H2-S1 (sail at $l_s = 50$ m) have very large difference (about 16.64%) suggesting that the location of sail has large influence on drag for the hull H2. This "hull-sail interaction" has been investigated by varying the sail location for both H1 and H2 hull shapes at $U = 10$ m/s and the results are plotted in Figure 9. This plot shows that hull–sail interaction is (1) very small for H1 in the entire range of sail location l_s (15–60 m), (2) small for H2 in $30\,\text{m} \leqslant l_s \leqslant 45\,\text{m}$ and (3) large for H2 in $l_s < 30$ m and $l_s > 45$ m. The very small hull–sail interaction is another positive feature of combined hull–sail optimization approach. Figure 10 presents the streamlines on the surface of both H1-S1 and H2-S2 for different locations of sail. From the

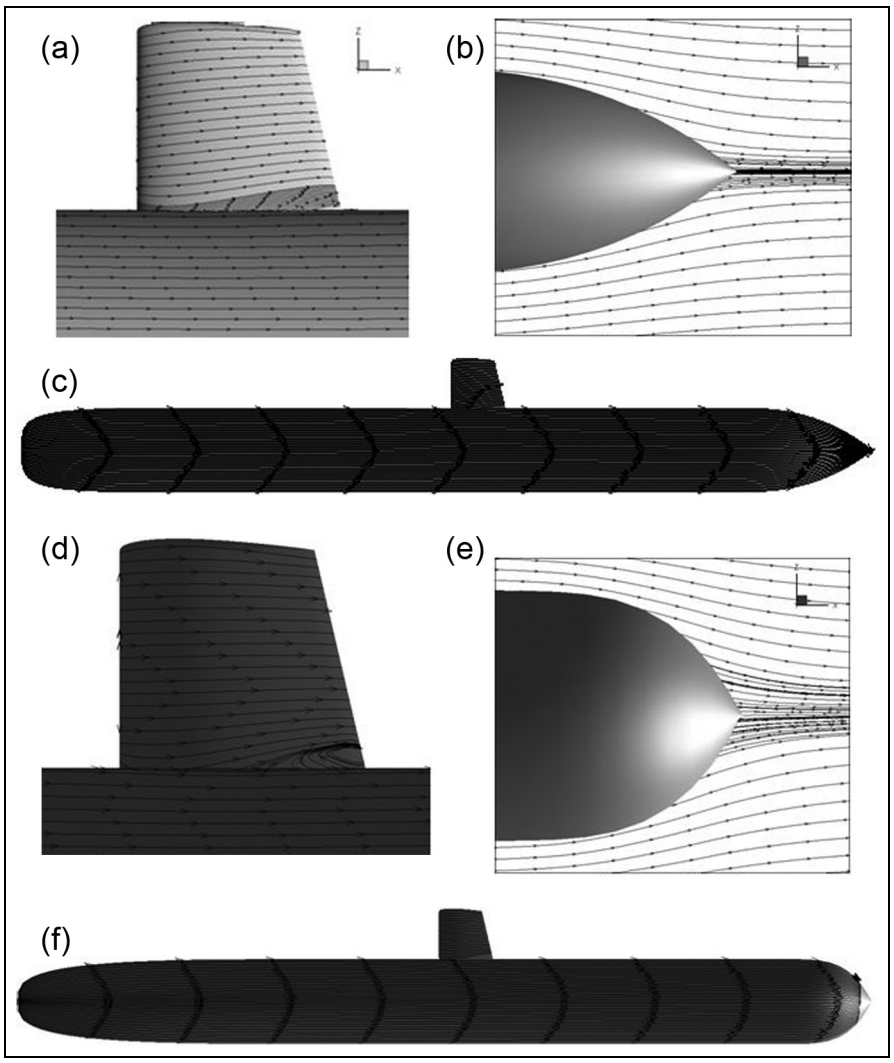

Figure 10. Streamlines on H1-S1 and H2-S2 with sail location at 40 m from nose tip ($U = 10$ m/s, 3.5 million cells): (a) at the location of sail (H1-S1), (b) at aft (H1-S1), (c) whole body (H1-S1), (d) at the location of sail (H2-S2), (e) at aft (H2-S2) and (f) whole body (H2-S2).

Table 3. The design parameters of four optimized designs.

Parameters	D1	D2	D3	D4
L_n (m)	18.541	18.548	6.523	21.777
L_m (m)	51.784	48.772	60.978	49.583
L_t (m)	9.675	12.68	12.499	8.64
L (m)	80	80	80	80
r_{max} (m)	3.997	3.994	3.993	3.96
n_n	4.86	4.81	2.39	2.36
n_t	2.71	2.53	1.78	3.37
l_s (m)	47.74	50	30.043	28.996
S (m^2)	1991.1	1962.19	1934.24	1913.6
∇ (m^3)	3743	3625	3608	3512
L/D_{max}	10	10.01	10.01	10.10
$\nabla^{2/3}/S$	0.12	0.12	0.12	0.12
Re_L (U)	6.37×10^8 (8 m/s)	7.96×10^8 (10 m/s)	9.56×10^8 (12 m/s)	1.19×10^9 (15 m/s)
D (N)	139,854	215,965	233,547	382,550

Table 4. Drag coefficients of the optimized hull shapes.

Configuration	Drag coefficients	U = 8 m/s	U = 10 m/s	U = 12 m/s	U = 15 m/s
D1	C_{DV}	0.01813	0.01893	0.01793	0.01774
	C_{FV} (% C_{DV})	55.8	55.4	54.9	54.3
	C_{PV} (% C_{DV})	44.2	44.6	45.1	45.7
D2	C_{DV}	0.01875	0.01831	0.01813	0.01797
	C_{FV} (% C_{DV})	58.1	57.5	56.9	56.5
	C_{PV} (% C_{DV})	41.9	42.5	43.1	43.5
D3	C_{DV}	0.01903	0.01950	0.01378	0.01607
	C_{FV} (% C_{DV})	65.1	64.5	63.9	63.5
	C_{PV} (% C_{DV})	34.9	35.5	36.1	36.5
D4	C_{DV}	0.01959	0.01949	0.01507	0.01471
	C_{FV} (% C_{DV})	58.4	57.8	57.6	57.3
	C_{PV} (% C_{DV})	41.6	42.2	42.4	42.7

figure, we can notice that for H2-S2 the vortices are created close to the intersection of the sail and the hull, whereas in the case of H1-S1 it is not. This may be one of the reasons why the drag for H2-S2 is high.

Optimization problems for a range of forward speeds

Since it is established that combined hull–sail optimization (problem P1) yields lowest drag shape, this optimization approach was carried out for four values of forward speed, namely, $U = 8$ m/s (U_1), 10 m/s (U_2), 12 m/s (U_3) and 15 m/s (U_4). The results for U_2 have already been discussed in section "Optimization problems P1, P2 and P3." For these four speeds, the hull shapes are picked from the optimal Pareto front such that the volumes of all the hulls are almost same (less than 3% of each other). The particulars of the four optimized hulls—denoted D1 for U_1, D2 for U_2, D3 for U_3 and D4 for U_4—are shown in Table 3. The design D_2 is same as the design H1-S1 discussed in section "Optimization problems P1, P2 and P3." The volumetric drag coefficients and the percentage contributions of viscous pressure drag and skin friction to the total drag are given in Table 4. In all designs, the skin friction drag dominates over the viscous pressure drag, being in the narrow range of 54.3%–65.1%. The optimized hull shapes, including the corresponding sail locations, of the four designs are shown in Figure 11.

One has to choose between designs D1–D4, each optimized for a particular forward speed, as the design of the submarine hull. To aid this process, Table 5 records the total drag of all these four designs (D1 to D4) at all four speeds (U_1 to U_4) which covers the operating speed range of the submarine. In Table 5, the excess drag (in %) of a design at a speed with respect to the drag of the optimized design for that speed are recorded. It is seen that the values of maximum excess drag of a design are 24.9% for D1, 24.2% for D2, 10.07% for D3 and 6.8% for D4. Therefore, design D4 will have minimum excess drag in the entire speed range. As a result, design D4 may be considered the optimized design of the submarine.

The wake fraction of the hull is an important parameter for the design of propeller. The steady-state RANS solver generated wake fractions (w) for the four designs are also presented in Table 5. It is seen that the optimum design D4 has the most favorable (i.e. highest) wake fraction at all four speeds, thus making it a good, if not optimum, design from the point of view of wake fraction also. Table 6 presents the drag values of

Table 5. Drag (D), wake fraction (w) and excess drag of a design at a speed with respect to the drag of the optimized design for that speed (values in %).

U (m/s)	D (N) (excess drag in %)				w			
	D1	D2	D3	D4	D1	D2	D3	D4
8	139,854 (0%)	141,592 (1.22%)	143,245 (2.4%)	144,833 (3.43%)	0.327	0.263	0.218	0.359
10	228,149 (5.3%)	215,965 (0%)	229,400 (5.85%)	225,231 (4.11%)	0.325	0.259	0.214	0.352
12	311,232 (24.9%)	308,127 (24.2%)	233,547 (0%)	250,758 (6.8%)	0.322	0.254	0.211	0.347
15	481,149 (20.4%)	477,033 (19.8%)	425,412 (10.07%)	382,550 (0%)	0.319	0.249	0.207	0.344

Table 6. Drag of hull shape of D4 for various locations of sail ($U = 15$ m/s).

l_s (m)	15	25	28.996	35	45	55	60
D (N)	385,880	384,840	382,550	385,342	388,340	383,260	386,450

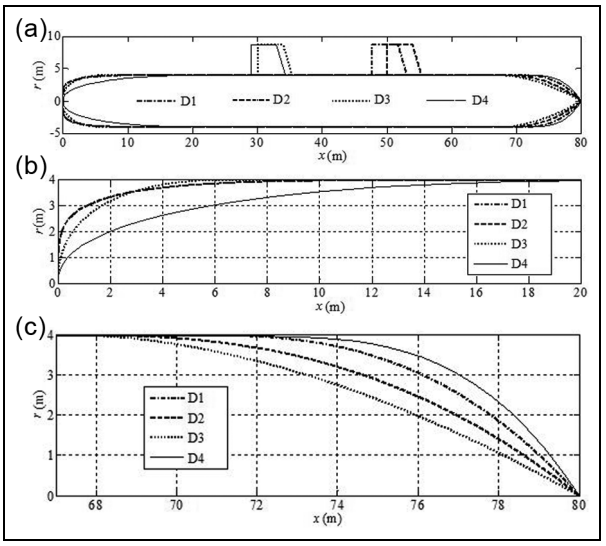

Figure 11. Geometries of the optimized shapes D1, D2, D3 and D4: (a) overall shapes, (b) nose shapes and (c) tail shapes.

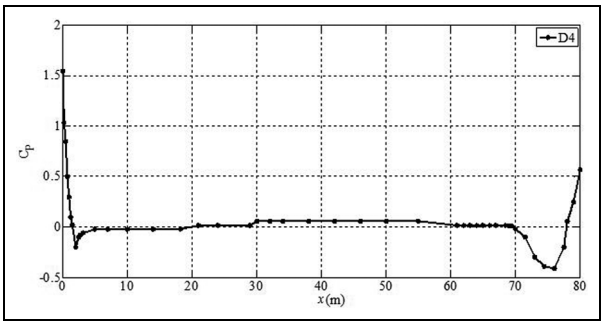

Figure 12. Variation of the pressure coefficient of D4 in $z = 0$ plane ($U = 15$ m/s).

the hull of the optimum design D4 for a range of sail locations from 15 to 60 m. It can be seen that the hull–sail interaction is negligibly small, and the maximum difference in drag with respect to the minimum value of the optimum design D4 is only about 1.5%. This was the conclusion for hull H1 also (which is same as that of D2) as shown in Figure 9. This implies that having obtained the optimum hull–sail combination from the optimization problem P1, one can locate the sail longitudinally almost anywhere without any appreciable additional drag, a fact which may be very useful in practice.

Figure 12 presents the pressure coefficient over length of the optimum design D4 in the plane $z = 0$. Figure 13 shows the velocity distributions in the boundary layer over the aft part of the optimized design D4 ($65\,\text{m} < x < 80\,\text{m}$) and also in its near wake (80–90 m). The asymmetry of the velocity profiles (in $y = 0$ plane) due to the presence of the sail structure is noticeable over the body. The velocity profiles, however, become symmetric in the wake. These two figures represent the key fluid dynamic characteristics of the flow around the submarine.

Conclusion

This article presents a NSGA-II-based multi-objective (drag and volume) optimization model integrated with CFD for shape design of submarine hull described by a simple 5-parameter formula. The shape of the sail is assumed fixed and hence is not a part of the optimization process but its longitudinal location over the submarine hull is an outcome of optimization. Two approaches to optimization are explored, one optimizes the combined "hull shape–sail location" and the other optimizes the hull shape first, and for this optimized hull shape, the sail location is optimized next. The former approach yields lower drag and negligibly small hull–sail interaction so that one has wider latitude to place the sail anywhere over the length of the submarine. This approach was chosen to obtain an optimum design considering the range of operating speed of the

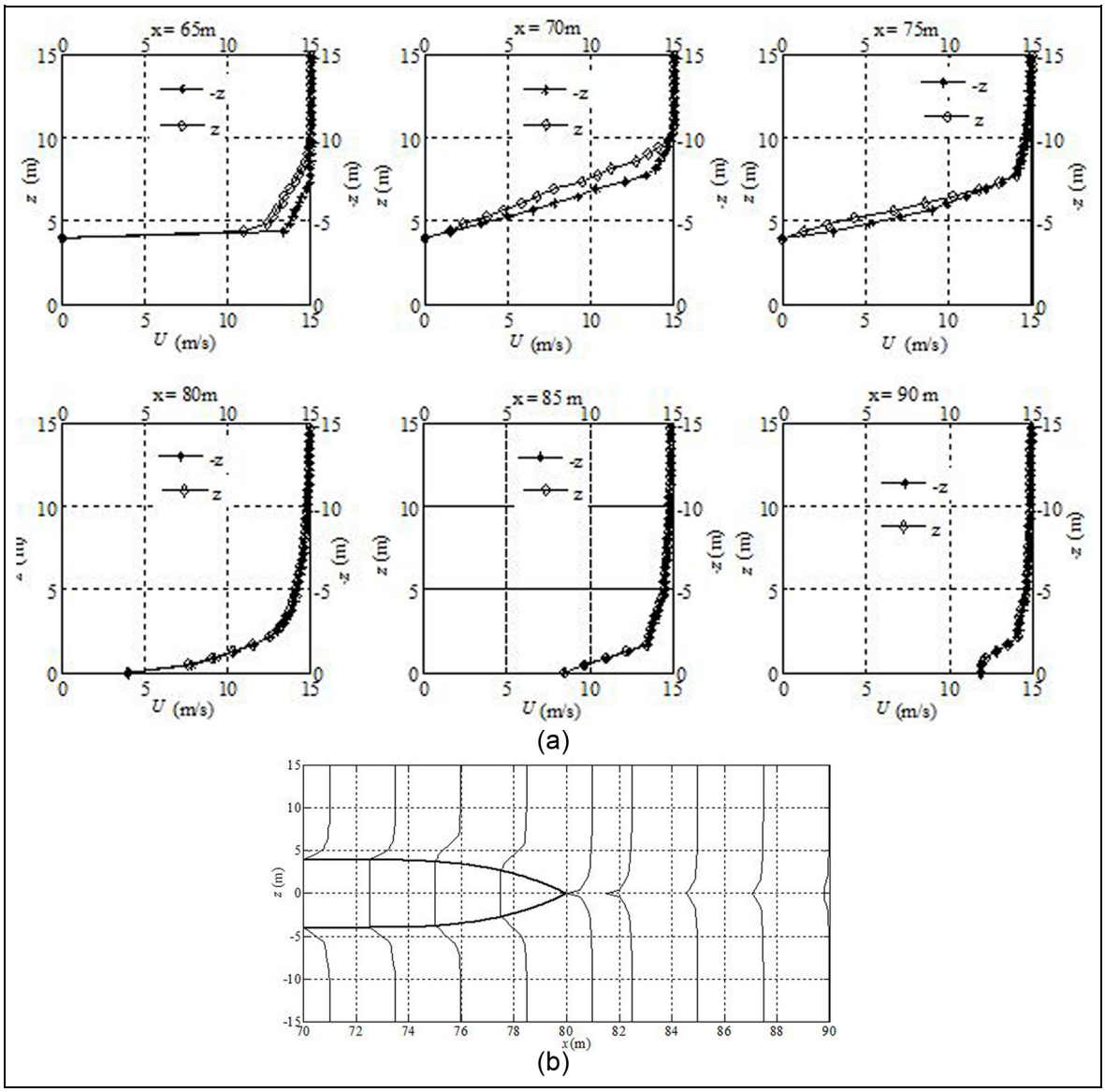

Figure 13. Velocity profiles of D4 for $U = 15$ m/s: (a) a few velocity profiles in +z and −z directions in $y = 0$ plane at aft and in the wake and (b) velocity profiles in $y = 0$ plane.

submarine. The GA and RANS solver are seamlessly integrated in a single code so that it becomes an effective computational tool for optimization. This approach can be extended to multi-objective problems that include wake fraction of the hull which is an important design parameter.

Declaration of Conflicting Interests

The author(s) declared no potential conflicts of interest with respect to the research, authorship and/or publication of this article.

Funding

The author(s) received no financial support for the research, authorship and/or publication of this article.

References

1. Parsons JS, Goodson RE and Goldschmied FR. Shaping of axisymmetric bodies for minimum drag in incompressible flow. *J Hydronaut* 1974; 8(3): 100–107.
2. Ray T, Gokarn RP and Sha OP. A global optimization model for ship design. *Comput Ind* 1995; 26: 175–192.
3. Warren CL. *Submarine design optimization using boundary layer control*. Naval Engineer Thesis, Department of Ocean Engineering and Master's Thesis, Department of Mechanical Engineering, Massachusetts Institute of Technology, Cambridge, MA, 1997.
4. Percival S, Hendrix D and Noblesse F. Hydrodynamic optimization of ship hull forms. *Appl Ocean Res* 2001; 23(6): 337–355.
5. Campana EF, Peri D, Tahara Y, et al. Shape optimization in ship hydrodynamics using computational fluid dynamics. *Comput Method Appl M* 2006; 196(1–3): 634–651.

6. Peri D and Campana EF. High-fidelity models and multiobjective global optimization algorithms in simulation-based design. *J Ship Res* 2005; 49(3): 159–175.
7. Tahara Y, Tohyama S and Katsui T. CFD-based multi-objective optimization method for ship design. *Int J Numer Method Fluid* 2006; 52: 499–527.
8. Demko D. *Tools for multi-objective and multi-disciplinary optimization in naval ship design*. MS Thesis, Virginia Polytechnic Institute and State University, Blacksburg, VA, 2006.
9. Hart CG and Vlahopoulos N. A multidisciplinary design optimization approach to relating affordability and performance in a conceptual submarine design. *J Ship Prod Des* 2010; 26(4): 273–289.
10. Shahid M and Huang D. Computational fluid dynamics based bulbous bow optimization using a genetic algorithm. *J Mar Sci Appl* 2012; 11: 286–294.
11. Paz MJD and Tascon OD. Multiobjective optimization of a submarine hull design. *Ship Sci Technol* 2013; 7: 27–42.
12. Bettle MC, Gerber AG and Watt GD. Unsteady analysis of the six DOF motion of a buoyantly rising submarine. *Comput Fluids* 2009; 38: 1833–1849.
13. Watt G. *Modelling and simulating unsteady six degrees-of-freedom submarine rising maneuvers*. Technical report DRDC Atlantic TR 2007-008, 1 February 2007. Ottawa, ON, Canada: Defence Research and Development Canada.
14. Mackay M. *The standard submarine model: a survey of static hydrodynamic experiments and semi-empirical predictions*. Technical report DRDC Atlantic TR 2003-079, June 2003. Ottawa, ON, Canada: Defence Research and Development Canada.
15. Vasudev KL, Sharma R and Bhattacharyya SK. A multi-objective optimization design framework integrated with CFD for the design of AUVs. *Method Oceanograph* 2014; 10: 138–165.
16. Alvarez A, Bertram V and Gualdesi L. Hull hydrodynamic optimization of autonomous underwater vehicles operating at snorkeling depth. *Ocean Eng* 2009; 36: 105–112.
17. Deb K, Pratap A, Agarwal S, et al. A fast and elitist multi-objective genetic algorithm: NSGA-II. *IEEE T Evolut Comput* 2002; 6(2): 182–197.
18. Deb K. *Multi-objective optimization using evolutionary algorithms*. Chichester: Wiley India Private Limited, 2014.
19. *Shipflow theoretical manual* (version 5.1). Göteborg: Flowtech International AB, 2007.
20. Michalewicz Z and Attia NF. Evolutionary optimization of constrained problems. In: *Proceedings of the 3rd annual conference on evolutionary programming* (ed AV Sebald and LJ Fogel), San Diego, CA, 24–26 February 1994, pp.98–108. River Edge, NJ: World Scientific Publishing.
21. Miettinen K, Makela MM and Toivanen J. Numerical comparison of some penalty-based constraint handling techniques in genetic algorithms. *J Global Optim* 2003; 27: 427–446.